

## Supporting Information

### **[(Me)<sub>2</sub>NH<sub>2</sub>]<sub>0.75</sub>[Ag<sub>1.25</sub>SnSe<sub>3</sub>]: A Three-dimensionally Microporous Chalcogenide Exhibiting Framework Flexibility Upon Ion-exchange**

By Jian-Rong Li and Xiao-Ying Huang\*

State Key Laboratory of Structural Chemistry, Fujian Institute of Research on the Structure of Matter, Chinese Academy of Sciences, Fuzhou, Fujian 350002, P. R.

China. Fax: (+86) 591-83793727

E-mail: [xyhuang@fjirsm.ac.cn](mailto:xyhuang@fjirsm.ac.cn)

(Jian-Rong Li ) Graduate School, Chinese Academy of Sciences  
Beijing 100039, P. R. China.

#### 1. More Structural details

The intensity data were collected on a Rigaku SCXmini CCD diffractometer for **1**, **1Cs**, **1Rb** and a Rigaku Mercury CCD diffractometer for **1NH<sub>4</sub>** with graphite-monochromated MoK $\alpha$  radiation ( $\lambda = 0.71073 \text{ \AA}$ ) at room temperature. The structures were solved by direct methods and refined by full-matrix least-squares on  $F^2$  using the SHELX97 program package.<sup>[1]</sup> The hydrogen atoms attached to the C and N atoms in compound **1** were located at geometrically calculated positions, and the restraints (DFIX, ISOR and SIMU) were applied on C and N atoms to obtain chemical-reasonable models for disordered dimethylammonium ions. The Cs1 ion in compound **1Cs** showed positional disorder and was refined split into three non-equivalent positions Cs1A, Cs1B and Cs1C, respectively, while the Cs2 ion was half-occupied. The water molecules are also half-occupied. The hydrogen atoms of the water molecules were not added. In the structure of **1Rb**, the Rb1 ion showed positional disorder and was refined split into two non-equivalent positions Rb1A and Rb1B, respectively, while the Rb2 ion was half-occupied. The residual dimethylammounium cations in **1Cs** and **1Rb** could not be found in the difference Fourier maps, therefore were not included in the structure refinements. In the structure of **1NH<sub>4</sub>**, the hydrogen atoms were not added, and the restraints (DFIX and SIMU) were applied on C and N atoms to obtain chemical-reasonable models for the disordered dimethylammonium ion. The empirical formulae for **1Cs**, **1Rb**, and **1NH<sub>4</sub>** were calculated based on the TGA, EA and EDS results. The crystal data and structure refinement details are listed in Table S1. The selected bond lengths and angles of compounds **1**, **1Cs**, **1Rb**, and **1NH<sub>4</sub>** are listed in Table S2.

[1] G. M. Sheldrick, *SHELXS97 and SHELXL97*, University of Göttingen, Germany, 1997.

**Table S1** Crystallographic data for compound **1** and the ion-exchanged products

	<b>1</b>	<b>1Cs</b>	<b>1Rb</b>	<b>1NH<sub>4</sub></b>
Formula	$[(\text{Me}_2\text{NH}_2)_{0.75}[\text{Ag}_{1.25}\text{SnSe}_3]]$	$[\text{Me}_2\text{NH}_2]_{0.05}\text{Cs}_{0.70}[\text{Ag}_{1.25}\text{SnSe}_3]\cdot0.25\text{H}_2\text{O}$	$[\text{Me}_2\text{NH}_2]_{0.10}\text{Rb}_{0.65}[\text{Ag}_{1.25}\text{SnSe}_3]\cdot0.75\text{H}_2\text{O}$	$[\text{Me}_2\text{NH}_2]_{0.25}(\text{NH}_4)_{0.50}[\text{Ag}_{1.25}\text{SnSe}_3]\cdot0.5\text{H}_2\text{O}$
Empirical formula	$\text{C}_{1.50}\text{H}_6\text{Ag}_{1.25}\text{N}_{0.75}\text{Se}_3\text{Sn}$	$\text{C}_{0.10}\text{H}_{0.90}\text{Ag}_{1.25}\text{Cs}_{0.70}\text{N}_{0.05}\text{O}_{0.25}\text{Se}_3\text{Sn}$	$\text{C}_{0.20}\text{H}_{2.30}\text{Ag}_{1.25}\text{N}_{0.10}\text{O}_{0.75}\text{Rb}_{0.65}\text{Se}_3\text{Sn}$	$\text{C}_{0.50}\text{H}_5\text{Ag}_{1.25}\text{N}_{0.75}\text{O}_{0.50}\text{S}_{\text{e}_3\text{Sn}}$
Crystal Size (mm)	$0.25\times0.16\times0.14$	$0.16\times0.14\times0.12$	$0.11\times0.10\times0.09$	$0.07\times0.06\times0.05$
Crystal system	tetragonal	tetragonal	tetragonal	tetragonal
Space group	<i>P-42</i> <sub>1</sub> <i>m</i>	<i>P-42</i> <sub>1</sub> <i>m</i>	<i>P-42</i> <sub>1</sub> <i>m</i>	<i>P-42</i> <sub>1</sub> <i>m</i>
<i>a</i> (Å)	13.8051(8)	13.9886(8)	13.998(2)	13.9087(6)
<i>c</i> (Å)	9.6707(9)	8.8534(13)	8.6852(17)	8.8618(7)
<i>V</i> (Å <sup>3</sup> )	1843.0(2)	1732.4(3)	1701.9(5)	1714.33(17)
<i>Z</i>	8	8	8	8
$\mu$ (mm <sup>-1</sup> )	17.113	21.097	22.227	18.400
<i>F</i> (000)	1848	2025	1960	1824
$\theta$ range (°)	2.57 to 27.46	2.72 to 27.47	2.76 to 27.49	2.73 to 27.46
Reflections measured	14465	13505	13288	13455
Independent reflections	2228	2105	2066	2056
Observed Reflection	2068	1886	1771	1973
[ $>2\sigma(I)$ ]				
Temperature (K)	293	293	293	293
$\rho_{\text{calc}}/\text{g cm}^{-3}$	3.784	4.526	4.403	4.029
Parameter	86	84	84	84
<i>R</i> <sub>int</sub>	0.0538	0.0598	0.0888	0.0648
<i>R</i> <sub>1</sub> , <i>wR</i> <sub>2</sub> [ $>2\sigma(I)$ ] <sup>a, b</sup>	0.0366, 0.0799	0.0520, 0.1423	0.0639, 0.1399	0.0465, 0.0910
<i>GOF</i>	1.074	1.081	1.084	1.152
Largest diff. Peak and hole/e Å <sup>-3</sup>	1.037, -1.006	2.021, -1.583	1.066, -1.083	0.961, -1.018

$$^a R_1 = \sum \|F_o\| - \|F_c\| / \sum \|F_o\|, \quad ^b wR_2 = [\sum w(F_o^2 - F_c^2)^2 / \sum w(F_o^2)]^{0.5}$$

**Table S2.** Selected bond lengths ( $\text{\AA}$ ) and angles ( $^\circ$ ) for **1** and the ion-exchanged products **1NH<sub>4</sub>**, **1Cs**, and **1Rb**.

	<b>1</b>	<b>1NH<sub>4</sub></b>		<b>1Cs</b>	<b>1Rb</b>
Sn(1)-Se(1)	2.4861(10)	2.4795(13)	Sn(1)-Se(1)	2.4804(16)	2.480(2)
Sn(1)-Se(2)	2.5064(11)	2.5040(14)	Sn(1)-Se(2)	2.5048(16)	2.501(2)
Sn(1)-Se(3)	2.5795(12)	2.5756(15)	Sn(1)-Se(3)	2.5809(19)	2.575(2)
Sn(1)-Se(4)	2.5595(11)	2.5701(14)	Sn(1)-Se(4)	2.5777(18)	2.570(2)
Ag(1)-Se(2)#1	2.5950(12)	2.5823(15)	Ag(1)-Se(2)#1	2.5782(18)	2.582(2)
Ag(1)-Se(1)	2.6281(13)	2.6151(17)	Ag(1)-Se(1)	2.620(2)	2.610(3)
Ag(1)-Se(2)#2	2.6554(13)	2.6687(17)	Ag(1)-Se(2)#2	2.672(2)	2.678(3)
Ag(1)-Ag(1)#1	3.1826(17)	3.208(2)	Ag(1)-Ag(1)#1	3.185(2)	3.208(3)
Ag(1)-Ag(1)#2	3.2414(16)	3.208(2)	Ag(1)-Ag(1)#2	3.221(3)	3.185(3)
Ag(1)-Ag(1)#3	3.2414(16)	3.228(2)	Ag(1)-Ag(1)#3	3.221(3)	3.185(3)
Ag(2)-Se(1)#1	2.6759(10)	2.6888(12)	Ag(2)-Se(1)	2.7022(15)	2.7012(19)
Ag(2)-Se(1)#4	2.6759(10)	2.6888(12)	Ag(2)-Se(1)#1	2.7022(15)	2.7012(19)
Ag(2)-Se(1)#5	2.6759(10)	2.6888(12)	Ag(2)-Se(1)#4	2.7022(15)	2.7012(19)
Ag(2)-Se(1)	2.6759(10)	2.6888(12)	Ag(2)-Se(1)#5	2.7022(15)	2.7012(19)
Se(1)-Sn(1)-Se(2)	119.59(4)	120.46(5)	Se(1)-Sn(1)-Se(2)	120.35(6)	120.31(7)
Se(1)-Sn(1)-Se(4)	108.84(4)	108.68(6)	Se(1)-Sn(1)-Se(4)	109.39(7)	109.77(9)
Se(2)-Sn(1)-Se(4)	108.72(5)	106.61(6)	Se(2)-Sn(1)-Se(4)	107.49(8)	105.97(10)
Se(1)-Sn(1)-Se(3)	114.21(5)	113.13(6)	Se(1)-Sn(1)-Se(3)	112.99(8)	112.06(10)
Se(2)-Sn(1)-Se(3)	106.95(4)	109.17(6)	Se(2)-Sn(1)-Se(3)	107.87(8)	110.18(10)
Se(4)-Sn(1)-Se(3)	95.85(3)	95.72(4)	Se(4)-Sn(1)-Se(3)	95.87(5)	95.49(7)
Se(2)#1-Ag(1)-Se(1)	123.55(5)	124.35(6)	Se(2)#1-Ag(1)-Se(1)	126.26(8)	125.40(9)
Se(2)#1-Ag(1)-Se(2)#2	116.98(4)	119.30(5)	Se(2)#1-Ag(1)-Se(2)#2	118.06(6)	119.79(7)
Se(1)-Ag(1)-Se(2)#2	114.76(4)	110.94(5)	Se(1)-Ag(1)-Se(2)#2	109.90(6)	108.83(8)
Se(1)#1-Ag(2)-Se(1)#4	105.209(19)	99.45(2)	Se(1)#1-Ag(2)-Se(1)#4	99.23(2)	98.67(3)
Se(1)#1-Ag(2)-Se(1)	118.38(4)	132.18(6)	Se(1)#1-Ag(2)-Se(1)	132.77(7)	134.30(8)
Se(1)#4-Ag(2)-Se(1)	105.209(19)	99.45(2)	Se(1)#4-Ag(2)-Se(1)	99.23(2)	98.67(3)
Se(1)#1-Ag(2)-Se(1)#5	105.209(19)	99.45(2)	Se(1)#1-Ag(2)-Se(1)#5	99.23(2)	98.67(3)
Se(1)#4-Ag(2)-Se(1)#5	118.38(4)	132.18(6)	Se(1)#4-Ag(2)-Se(1)#5	132.79(7)	134.30(8)
Se(1)-Ag(2)-Se(1)#5	105.209(19)	99.45(2)	Se(1)-Ag(2)-Se(1)#5	99.23(2)	98.67(3)
Ag(1)-Se(1)-Ag(2)	97.87(4)	87.76(4)	Ag(1)-Se(1)-Ag(2)	86.36(5)	85.38(7)
Sn(1)-Se(1)-Ag(2)	103.02(3)	96.50(4)	Sn(1)-Se(1)-Ag(2)	97.02(5)	95.81(6)
Sn(1)-Se(1)-Ag(1)	83.06(4)	84.56(5)	Sn(1)-Se(1)-Ag(1)	84.38(6)	85.49(7)
Ag(1)#1-Se(2)-Ag(1)#3	76.24(4)	75.30(6)	Ag(1)#1-Se(2)-Ag(1)#3	75.65(7)	74.49(8)
Sn(1)-Se(2)-Ag(1)#1	104.35(4)	106.35(5)	Sn(1)-Se(2)-Ag(1)#1	106.02(6)	106.38(8)
Sn(1)-Se(2)-Ag(1)#3	96.81(4)	94.25(5)	Sn(1)-Se(2)-Ag(1)#3	94.69(6)	93.33(7)
Symmetry codes: #1 -x, -y, z; #2 y, -x, -z+1; #3 -y, x, -z+1; #4 -y, x, -z+2; #5 y, -x, -z+2.		Symmetry codes: #1 -x+1, -y+1, z; #2 -y+1, x, -z+1; #3 y, -x+1, -z+1; #4 y, -x+1, -z; #5 -y+1, x, -z.			

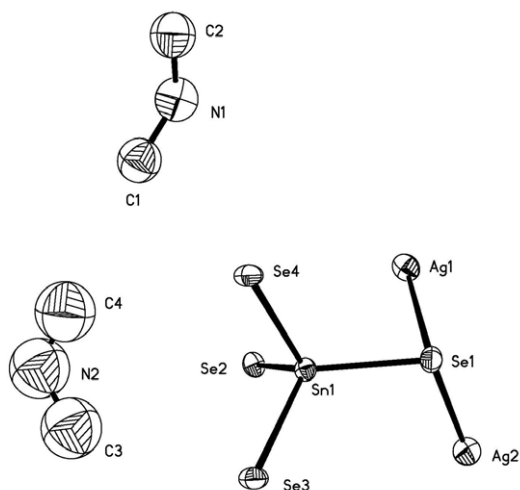


**Fig. S1** ORTEP plot showing the crystallographically asymmetric unit in the compound 1; thermal ellipsoids are given at the 30% probability level.

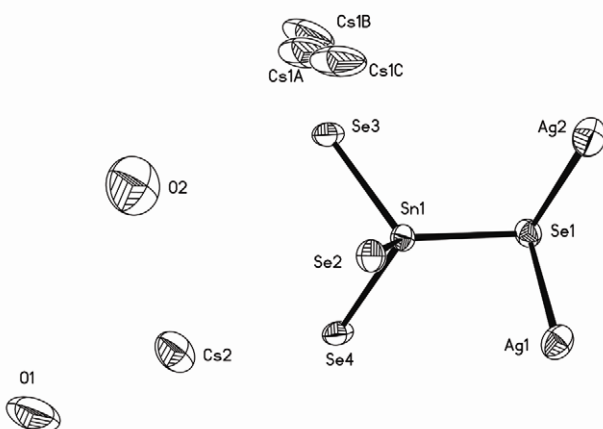


**Fig. S2** ORTEP plot showing the crystallographically asymmetric unit in the compound 1Cs; thermal ellipsoids are given at the 30% probability level.

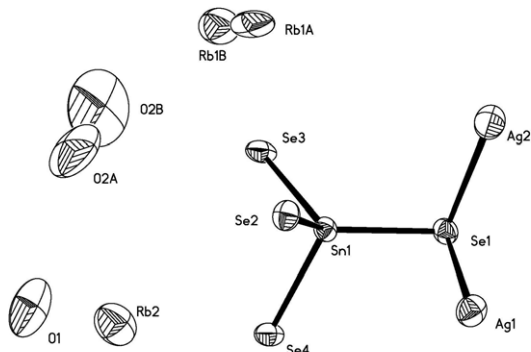


**Fig. S3** ORTEP plot showing the crystallographically asymmetric unit in the compound 1Rb; thermal ellipsoids are given at the 30% probability level.

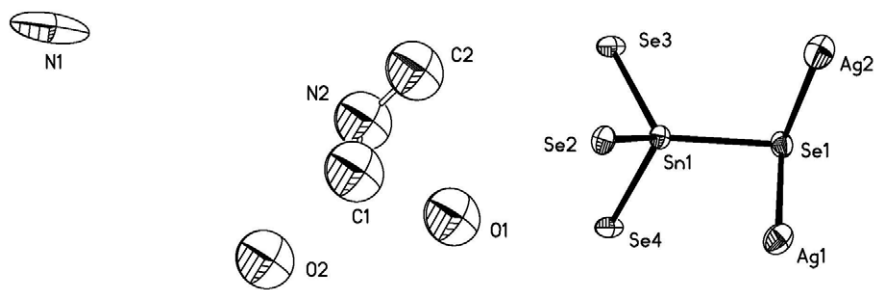


**Fig. S4** ORTEP plot showing the crystallographically asymmetric unit in the compound **1NH<sub>4</sub>**; thermal ellipsoids are given at the 30% probability level.

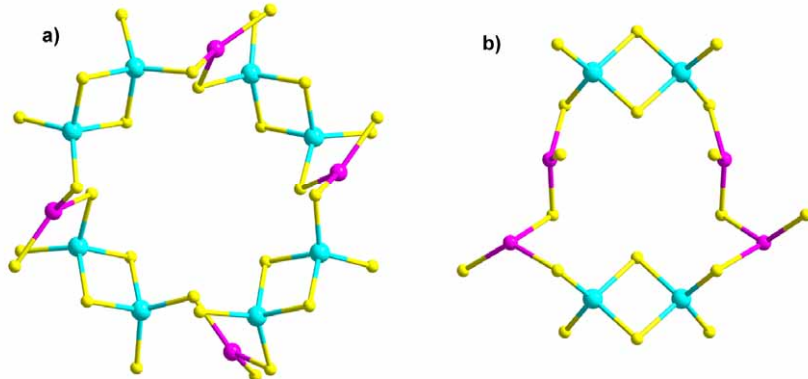


**Fig. S5** View of (a) the 24-membered ring window of the channel in the compound **1** along the *c* axis, and (b) the 16-membered ring window of the channel along the [110] direction. The Sn, Ag, Se atoms are drawn as turquoise, pink, and yellow balls, respectively.

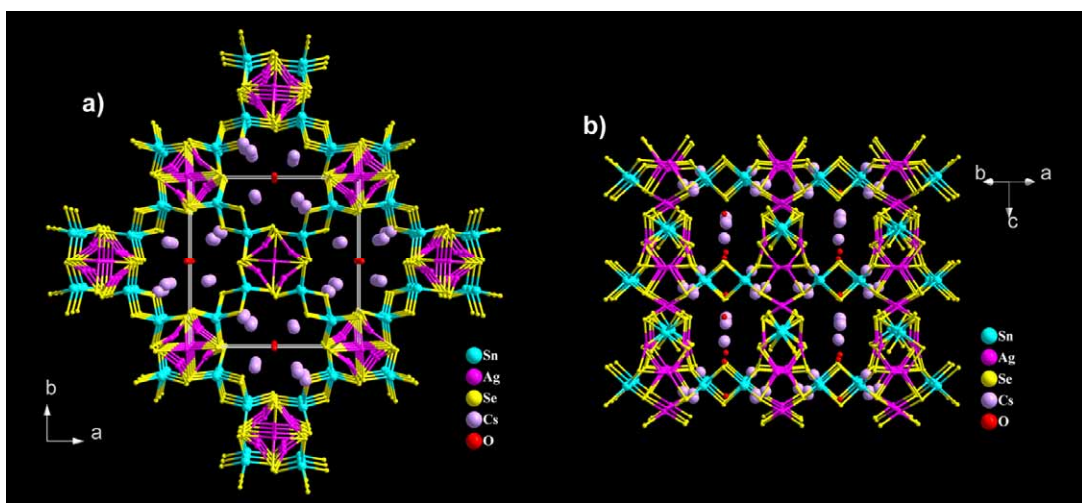


**Fig. S6** View of the structure of Cs-exchanged product (**1Cs**) along the *c* axis (a) and [110] direction (b).

## 2. Physical measurements

All chemicals employed in this study were analytical reagents and commercially available without further purification, except that AgCl was synthesized by the reaction of AgNO<sub>3</sub> and KCl. Microprobe elemental analyses were performed by using a field-emission scanning electron microscope (FESEM, JSM6700F) equipped with an energy-dispersive X-ray spectroscope (EDS, Oxford INCA). C, H and N analyses were performed on a German Elementary Vario EL III instrument. Powder X-ray diffraction (PXRD) patterns were recorded on a Rigaku MiniFlex II using CuK $\alpha$  radiation. Optical diffuse reflectance spectra were measured at room temperature with a Perkin-Elmer Lambda 900 UV/Vis spectrophotometer. A BaSO<sub>4</sub> plate was used as a standard (100% reflectance). The absorption spectra were calculated from reflectance spectra by using the Kubelka–Munk function:  $a/S = (1-R)^2/2R$ ,<sup>[1]</sup> where  $a$  is the absorption coefficient,  $S$  is the scattering coefficient which is practically independent of wavelength when the particle size is larger than 5  $\mu\text{m}$ , and  $R$  is the reflectance. Thermogravimetric analyses were carried out using crystalline samples loaded in Al<sub>2</sub>O<sub>3</sub> crucibles with a NETZSCH STA 449F3 unit at a heating rate of 5 °C/min under a nitrogen atmosphere.

[1] W. M. Wendlandt, H. G. Hecht, *Reflectance Spectroscopy*, Interscience, New York, **1966**.

### 2a). Elemental analyses

**Table S3.** Elemental analyses of **1** and the ion-exchange products

Exchanged Cations	EDS result	N, C, H, analysis (%) (Calc.)	Estimated formula	Exchange yield (%)
compound <b>1</b>	Ag <sub>1.24</sub> SnSe <sub>2.83</sub>	1.86, 3.43, 1.02 (2.00, 3.42, 1.14)	/	/
Cs <sup>+</sup>	Sn <sub>0.94</sub> Ag <sub>1.18</sub> Se <sub>3</sub> Cs <sub>0.70</sub>	0.3<, 0.3<, 0.3< (0.12 0.20 0.15)	[SnAg <sub>1.25</sub> Se <sub>3</sub> ][Me <sub>2</sub> NH <sub>2</sub> ] <sub>0.05</sub> Cs <sub>0.70</sub> ·0.25H <sub>2</sub> O	93
Rb <sup>+</sup>	Ag <sub>1.32</sub> SnSe <sub>3.19</sub> Rb <sub>0.65</sub>	0.3< 0.5, 0.62 (0.25, 0.43, 0.41)	[Me <sub>2</sub> NH <sub>2</sub> ] <sub>0.10</sub> Rb <sub>0.65</sub> [Ag <sub>1.25</sub> SnSe <sub>3</sub> ]·0.75H <sub>2</sub> O	87
NH <sub>4</sub> <sup>+</sup>	/	1.81, 1.08, 0.72 (2.02, 1.16, 0.97)	[Me <sub>2</sub> NH <sub>2</sub> ] <sub>0.25</sub> (NH <sub>4</sub> ) <sub>0.50</sub> [Ag <sub>1.25</sub> SnSe <sub>3</sub> ]·0.5H <sub>2</sub> O	67

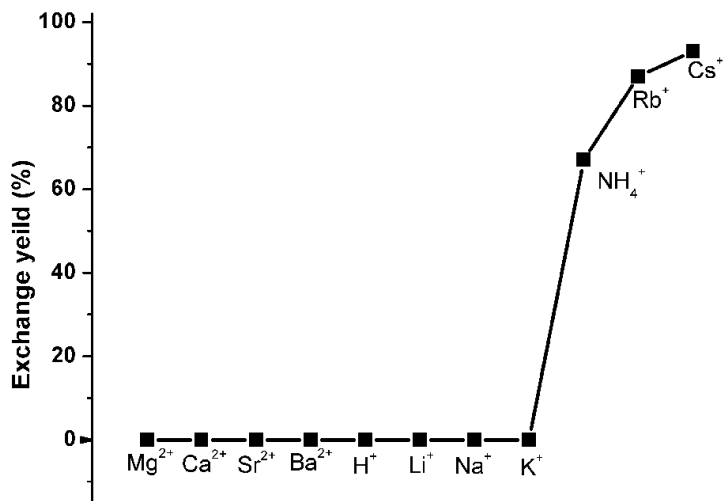


**Fig. S7.** The Cs<sup>+</sup>, Rb<sup>+</sup>, K<sup>+</sup>, Na<sup>+</sup>, Li<sup>+</sup>, H<sup>+</sup>, Ba<sup>2+</sup>, Sr<sup>2+</sup>, Ca<sup>2+</sup>, Mg<sup>2+</sup> and NH<sub>4</sub><sup>+</sup> ion-exchanged yields for the single ion-exchange experiments are plotted.

**Table S4.** Elemental analysis results for various single-ion-exchanged products‡

Exchanged Cation	EDS result
K <sup>+</sup>	Ag <sub>1.40</sub> SnSe <sub>3.30</sub>
Na <sup>+</sup>	Ag <sub>1.37</sub> SnSe <sub>2.90</sub>
Li <sup>+</sup>	Ag <sub>1.32</sub> SnSe <sub>3.15</sub>
Ba <sup>2+</sup>	Ag <sub>1.28</sub> SnSe <sub>3.21</sub>
Sr <sup>2+</sup>	Ag <sub>1.23</sub> SnSe <sub>3.20</sub>
Ca <sup>2+</sup>	Ag <sub>1.33</sub> SnSe <sub>3.09</sub>
Mg <sup>2+</sup>	Ag <sub>1.37</sub> SnSe <sub>2.90</sub>

‡ The results of TGA and EA for the H<sup>+</sup> exchanged products are in accordance with those of the pristine, indicating that no H<sup>+</sup> was exchanged.

2b) PXRD

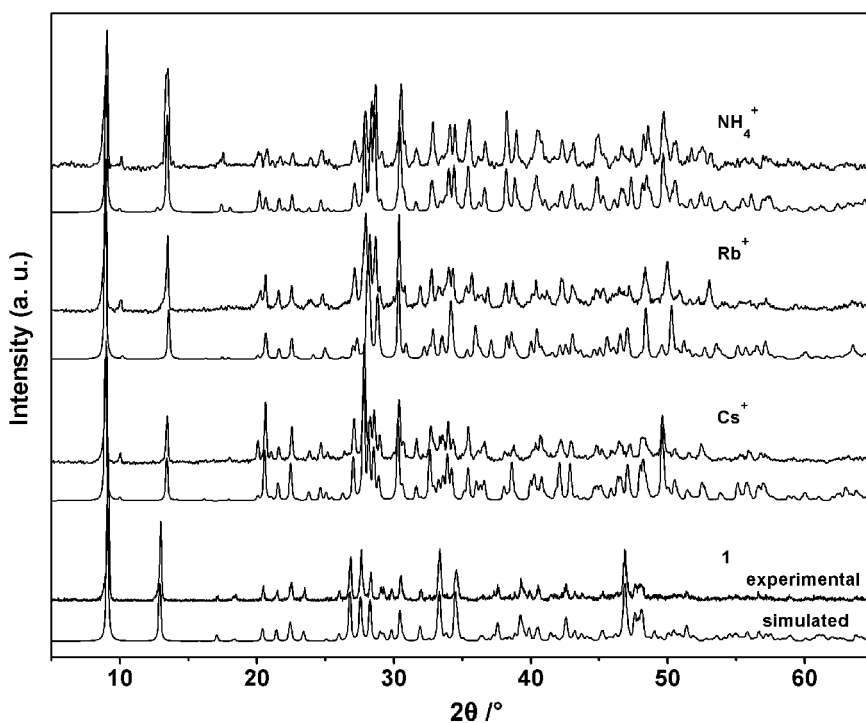


**Fig. S8.** The experimental PXRD patterns of the pristine compound **1**,  $\text{Cs}^+$ ,  $\text{Rb}^+$  and  $\text{NH}_4^+$ -exchanged products (top) are comparable with the simulated PXRD patterns (bottom) calculated from the respective single crystal X-ray data of **1**, **1Cs**, **1Rb** and **1NH<sub>4</sub>**.

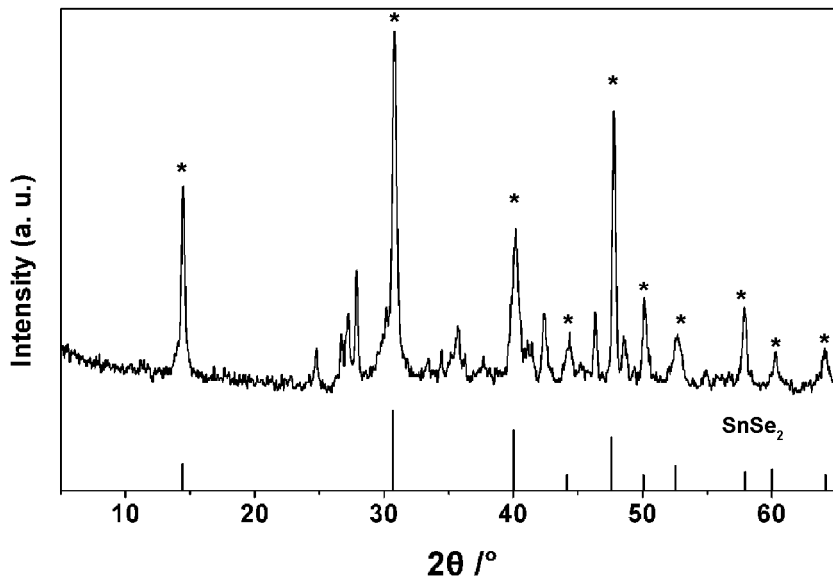


**Fig. S9** The PXRD pattern for the post-TGA residue of compound **1** after heated to 320 °C, identified as a mixture of  $\text{SnSe}_2$  and an indefinite powder.

## 2c) Optical absorption properties

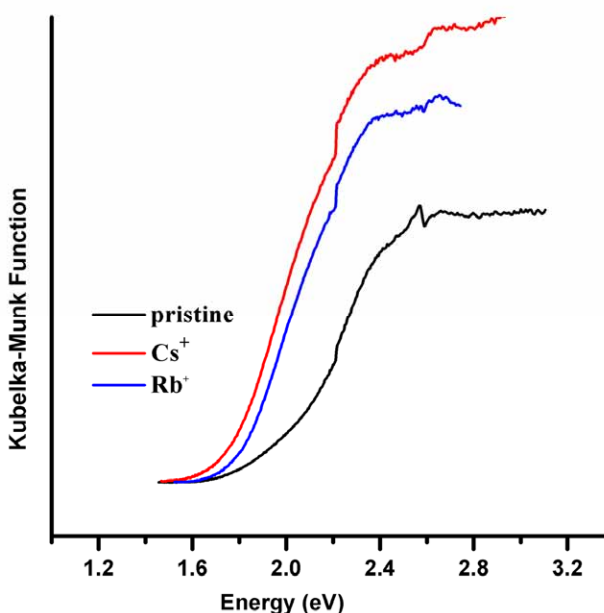


**Fig. S10** Optical absorption spectra for the pristine compounds **1**, Cs<sup>+</sup> and Rb<sup>+</sup>-exchanged products.

## 2d) TGA

The ion-exchange properties of **1** were further confirmed by thermogravimetric analyses (Fig. S11, and Tables S5). The thermal stabilities of **1** and ion-exchanged products were investigated on crystalline samples in a N<sub>2</sub> atmosphere from ~20 to 320°C. The TGA curve of **1** showed an obvious weight loss of 11.8% from 200–270°C, which could be attributed to the loss of dimethylammonium ions and the H<sub>2</sub>Se molecule (calcd. 12.2%). The post-TGA residue of **1** was identified as a mixture of SnSe<sub>2</sub> and an indefinite powder by powder X-ray diffraction (Fig. S9). The TGA curves of the Cs<sup>+</sup>- and Rb<sup>+</sup>-exchanged products displayed respective weight losses of solvents/water, unexchanged dimethylammonium ions and H<sub>2</sub>Se molecules, while the weight losses of NH<sub>4</sub><sup>+</sup>-exchanged products included lattice water, NH<sub>4</sub><sup>+</sup>, unexchanged diemethylammonium ions, and H<sub>2</sub>Se, respectively. All the observed weight losses of ion-exchanged products are close to the theoretical values. These results further support the ion-exchange properties of **1**.

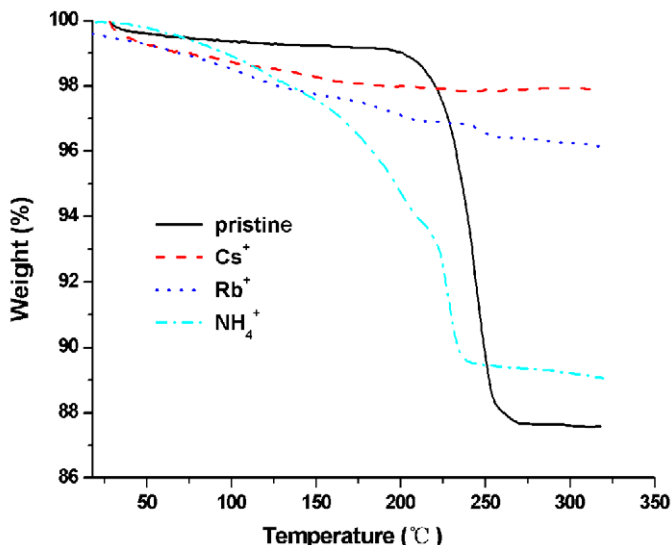


**Fig. S11** TGA curves of the products before and after the ion-exchange experiments.

**Table S5.** Detailed reports on the TGA results of the Cs<sup>+</sup>- Rb<sup>+</sup>- and NH<sub>4</sub><sup>+</sup>-exchanged products.

Exchanged cation	Estimated formula	Experimental weight loss at ~20-320°C	Calculated weight loss
Pristine	$[(\text{Me}_2\text{NH}_2)]_{0.75}[\text{Ag}_{1.25}\text{SnSe}_3]$	11.8% (0.75 Me <sub>2</sub> NH <sub>2</sub> + 0.375 H <sub>2</sub> Se)	12.3%
Cs <sup>+</sup>	$[\text{Me}_2\text{NH}_2]_{0.05}\text{Cs}_{0.70}[\text{Ag}_{1.25}\text{SnSe}_3]\cdot0.25\text{H}_2\text{O}$	1.4% (water) 0.4% (Me <sub>2</sub> NH <sub>2</sub> + H <sub>2</sub> Se)	0.8% 0.4%
Rb <sup>+</sup>	$[\text{Me}_2\text{NH}_2]_{0.10}\text{Rb}_{0.65}[\text{Ag}_{1.25}\text{SnSe}_3]\cdot0.75\text{H}_2\text{O}$	1.9 % (0.75 H <sub>2</sub> O) 1.3% (0.1 Me <sub>2</sub> NH <sub>2</sub> + 0.05 H <sub>2</sub> Se) 1.4% (0.5 H <sub>2</sub> O)	2.4% 1.5% 1.7%
NH <sub>4</sub> <sup>+</sup>	$[\text{Me}_2\text{NH}_2]_{0.25}(\text{NH}_4)_{0.50}[\text{Ag}_{1.25}\text{SnSe}_3]\cdot0.5\text{H}_2\text{O}$	4.8% (0.5 NH <sub>4</sub> <sup>+</sup> + 0.25 H <sub>2</sub> Se) 4.6% (0.25 Me <sub>2</sub> NH <sub>2</sub> + 0.125 H <sub>2</sub> Se)	5.6% 4.1%

### 3. Dehydration and re-hydration process

Single crystal x-ray analyses and elemental analyses indicated that the ion-exchanged products **1Cs**, **1Rb**, and **1NH<sub>4</sub>** all contain a small amount of lattice water molecules. To investigate if they are thermal stable after dehydration process, the crystalline samples of **1Cs** and **1Rb** were loaded in Al<sub>2</sub>O<sub>3</sub> crucibles and were heated in a NETZSCH STA 449F3 unit at a heating rate of 5 °C/min from room temperature (~20 °C) to 170 °C in a N<sub>2</sub> atmosphere, and then were kept in the unit at 170°C for 20 minutes to assure the removal of lattice water molecules. After cooled to room temperature, the powder x-ray diffraction experiments were performed on the residuals, which indicated that both the residuals of **1Cs** and **1Rb** after dehydration are still crystalline and the framework structures remain intact after the lattice water molecules being removed. Then the residuals were re-hydrated by immersed in water for six hours. TGA from room temperature (~20 °C) to 170 °C for the re-hydrated samples clearly suggested that the water molecules completely came back to the lattices of **1Cs** and **1Rb**, indicating the reversibility of the dehydration and re-hydration processes. All the results were depicted in Figs. S12 to S15.

To explore if the **1NH<sub>4</sub>** compound is stable after removing lattice water molecules and partial NH<sub>4</sub> ions, the crystalline sample of **1NH<sub>4</sub>** was loaded in Al<sub>2</sub>O<sub>3</sub> crucibles and were heated in a NETZSCH STA 449F3 unit at a heating rate of 5 °C/min from room temperature (~20 °C) to 200 °C in a N<sub>2</sub> atmosphere, and then were kept in the unit at 200°C for 20 minutes (Fig. S16). After cooled to room temperature, the powder x-ray diffraction experiment was performed on the residue, which showed extra peaks compared to that of the **1NH<sub>4</sub>** (Fig. S17). This suggested that **1NH<sub>4</sub>** is unstable after removal of lattice water molecules and partial NH<sub>4</sub> ions.

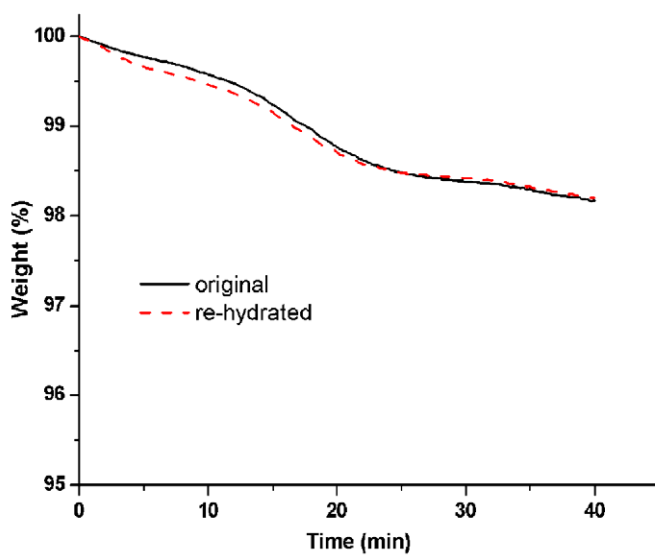


**Fig. S12** The TG curves for the dehydration-rehydration processes of **1Cs**. The black curve showed the dehydration process of the original sample **1Cs**. The red curve showed the dehydration process of the rehydrated sample of **1Cs** after immersed in water for six hours.

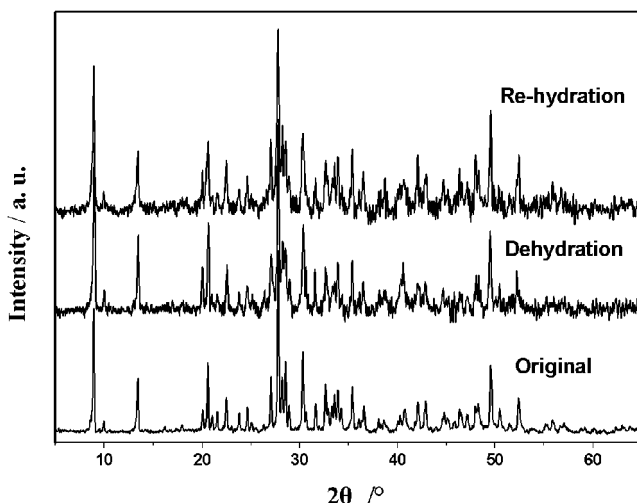


**Fig. S13** Comparison of the PXRD patterns of **1Cs** (bottom), dehydrated **1Cs** after heated at 170 °C for approximate 20 mins (middle) and the rehydrated **1Cs** after immersed in water for six hours (top).

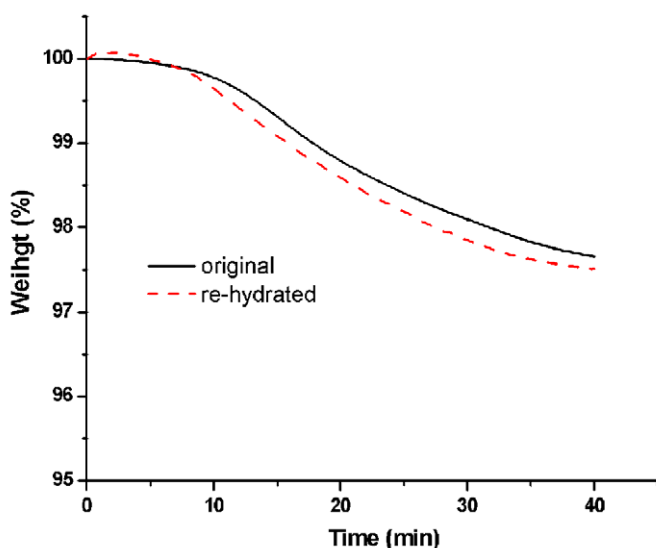


**Fig. S14** The TG curves for the dehydration-rehydration processes of **1Rb**. The black curve showed the dehydration process of the original sample **1Rb**. The red curve showed the dehydration process of the rehydrated sample of **1Rb** after immersed in water for six hours.

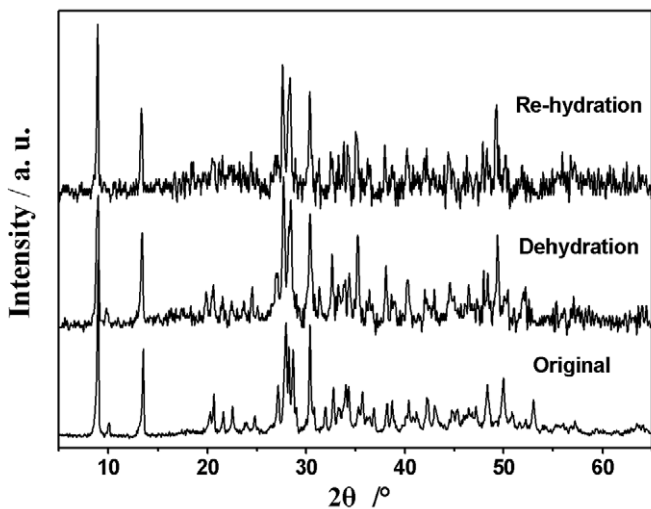


**Fig. S15** Comparison of the PXRD patterns of **1Rb** (bottom), dehydrated **1Rb** after heated at 170 °C for approximate 20 mins (middle) and the rehydrated **1Rb** (top) after immersed in water for six hours.

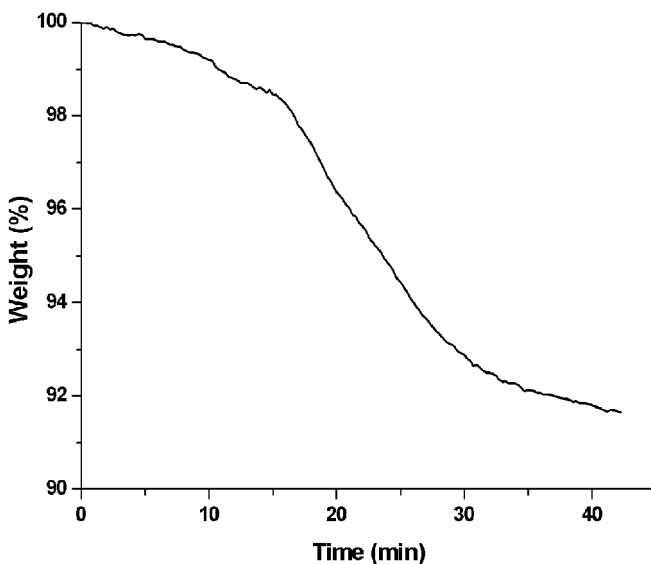


**Fig. S16** TG curve showing the removal of H<sub>2</sub>O and partial NH<sub>4</sub><sup>+</sup> of **1NH<sub>4</sub>** by heating at 200 °C for approximate 20 minutes.

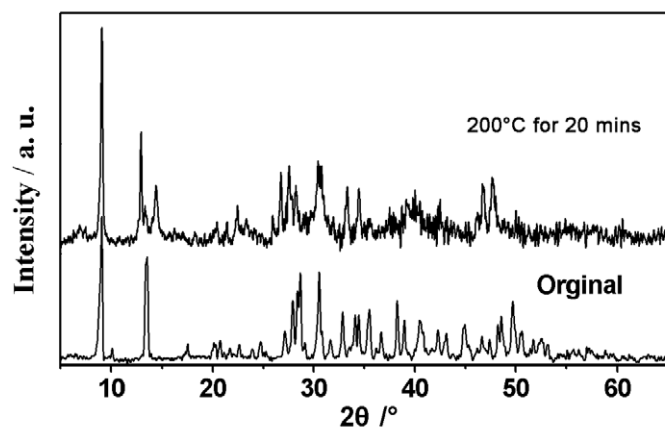


**Fig. S17** Comparison of the room temperature PXRD patterns of **1NH<sub>4</sub>** (bottom) and that of the residue of **1NH<sub>4</sub>** right after heated at 200 °C for approximate 20 minutes (top).